

1 **Evidence of cryptic methane cycling and non-methanogenic**
2 **methylamine consumption in the sulfate-reducing zone of**
3 **sediment in the Santa Barbara Basin, California**

4 Sebastian J.E. Krause^{1*#}, Jiarui Liu¹, David J. Yousavich¹, DeMarcus Robinson², David W.
5 Hoyt³, Qianhui Qin⁴, Frank Wenzhoefer^{5,6,7}, Felix Janßen^{5,6}, David L. Valentine⁸, and Tina
6 Treude^{1,2*}

7 ¹Department of Earth Planetary and Space Sciences, University of California, Los Angeles, CA
8 90095, USA

9 ²Department of Atmospheric and Ocean Sciences, University of California, Los Angeles, CA
10 90095, USA

11 ³Pacific Northwest National Laboratory Environmental and Molecular Sciences Division,
12 Richland, WA 99352, USA

13 ⁴Interdepartmental Graduate Program in Marine Science, University of California, Santa
14 Barbara, CA 93106, USA

15 ⁵HGF-MPG Group for Deep-Sea Ecology and Technology, Alfred-Wegener-Institute,
16 Helmholtz-Center for Polar and Marine Research, Am Handelshafen 12, 27570 Bremerhaven,
17 Germany

18 ⁶Max Planck Institute for Marine Microbiology, Celsiusstrasse 1, 28359 Bremen, Germany

19 ⁷Department of Biology, DIAS, Nordcee and HADAL Centres, University of Southern
20 Denmark, 5230 Odense M, Denmark

21 ⁸Department of Earth Science and Marine Science Institute, University of California Santa
22 Barbara, Santa Barbara, CA 93106, USA

23 *Correspondence: Sebastian Krause (sjkrause@ucsb.edu), Tina Treude (ttreude@g.ucla.edu)

24 **# Present address: Earth Research Institute, 6832 Ellison Hall, University of California**
25 **Santa Barbara, Ca 93106-3060**

26 **Abstract.** The recently discovered cryptic methane cycle in the sulfate-reducing zone of marine
27 and wetland sediments couples methylotrophic methanogenesis to anaerobic oxidation of
28 methane (AOM). Here we present evidence of cryptic methane cycling activity within the
29 upper regions of the sulfate-reducing zone, along a depth transect within the Santa Barbara
30 Basin, off the coast of California, USA. The top 0-20 cm of sediment from each station was
31 subjected to geochemical analyses and radiotracer incubations using $^{35}\text{S-SO}_4^{2-}$, ^{14}C -mono-
32 methylamine, and $^{14}\text{C-CH}_4$ to find evidence of cryptic methane cycling. Methane
33 concentrations were consistently low (3 to 16 μM) across the depth transect, despite AOM rates
34 increasing with decreasing water depth (from max $0.05 \text{ nmol cm}^{-3} \text{ d}^{-1}$ at the deepest station to
35 max $1.8 \text{ nmol cm}^{-3} \text{ d}^{-1}$ at the shallowest station). Porewater sulfate concentrations remained
36 high (23mM to 29 mM), despite the detection of sulfate reduction activity from $^{35}\text{S-SO}_4^{2-}$ -
37 incubations with rates up to $134 \text{ nmol cm}^{-3} \text{ d}^{-1}$. Metabolomic analysis showed that substrates
38 for methanogenesis (i.e., acetate, methanol and methylamines) were mostly below the detection
39 limit in the porewater, but some samples from the 1-2 cm depth section showed non-
40 quantifiable evidence of these substrates, indicating their rapid turnover. Estimated
41 methanogenesis from mono-methylamine ranged from 0.2 nmol to $0.5 \text{ nmol cm}^{-3} \text{ d}^{-1}$.
42 Discrepancies between the rate constants (K_1) of methanogenesis (from ^{14}C - mono-
43 methylamine) and AOM (from either ^{14}C - mono-methylamine-derived $^{14}\text{C-CH}_4$ or from
44 directly injected $^{14}\text{C-CH}_4$) suggest the activity of a separate, concurrent metabolic process
45 directly metabolizing mono-methylamine to inorganic carbon. We conclude that the results
46 presented in this work show strong evidence of cryptic methane cycling occurring within the
47 top 20 cm of sediment in the Santa Barbara Basin. The rapid cycling of carbon between
48 methanogenesis and methanotrophy likely prevents major build-up of methane in the sulfate-
49 reducing zone. Furthermore, our data suggest that methylamine is utilized by both
50 methanogenic archaea capable of methylotrophic methanogenesis and non-methanogenic

Deleted: ~

Deleted: ~

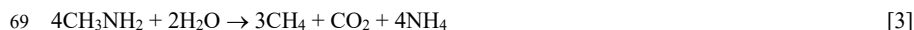
Deleted: ~

Deleted: ~

55 microbial groups. We hypothesize that sulfate reduction is responsible for the additional
56 methylamine turnover but further investigation is needed to elucidate this metabolic activity.
57

58 **1. Introduction**

59 In anoxic marine sediment, methane is produced by microbial methanogenesis in the
60 last step of organic carbon remineralization (Stephenson and Stickland, 1933; Thauer, 1998;
61 Reeburgh, 2007). This methane is produced by groups of obligate anaerobic methanogenic
62 archaea across the Euryarchyota, Crenarchaeota, Halobacterota, and Thermoplasmata phyla
63 (Lyu et al., 2018). Methanogens can produce methane through three different metabolic
64 pathways, using CO₂ (CO₂ reduction; e.g., hydrogenotrophic) (Eq. 1), acetate (acetoclastic)
65 (Eq. 2) and methylated substrates such as, methyl sulfides, methanol, and methylamines
66 (methylotrophic) (e.g., Eq. 3).



70 Classically, hydrogenotrophic and acetoclastic methanogenesis are dominant in deeper
71 sulfate-free sediment (Jørgensen, 2000; Reeburgh, 2007). This distinct geochemical zonation
72 is due to the higher free energy gained by sulfate-reducing bacteria within the sulfate reduction
73 zone coupling sulfate reduction with hydrogen and/or acetate consumption in sulfate-rich
74 sediment. Thus, sulfate-reducing bacteria tend to outcompete methanogenic archaea for
75 hydrogen and acetate in shallower sediment layers in the presence of sulfate (Kristjansson et
76 al., 1982; Winfrey and Ward, 1983; Lovley and Klug, 1986; Jørgensen, 2000). However,
77 methylotrophic methanogenesis is known to occur within the sulfate-reducing zone. The
78 activity of this process in the presence of sulfate reduction is possible because methylated
79 substrates, such as methylamines, are non-competitive carbon sources for methanogens
80 (Oremland and Taylor, 1978; Lovley and Klug, 1986; Maltby et al., 2016; Zhuang et al., 2016;
81 2018; 2018; Krause and Treude, 2021). Methylotrophic methanogenesis activity in the sulfate-
82 reducing zone has been detected in a wide range of aquatic environments, such as coastal
83 wetlands (Oremland et al., 1982; Oremland and Polcin, 1982; Krause and Treude, 2021),

84 upwelling regions (Maltby et al., 2016), and eutrophic shelf sediment (Maltby et al., 2018; Xiao
85 et al., 2018). Despite methylotrophic activity in the sulfate-reducing zone, methane
86 concentrations are several orders of magnitude lower than methane concentrations found in
87 deeper sediment zones where sulfate concentrations are depleted (Barnes and Goldberg, 1976;
88 Dale et al., 2008b; Wehrmann et al., 2011; Beulig et al., 2018).

89 In anoxic marine sediment, anaerobic oxidation of methane (AOM) is an important
90 methane sink that is typically coupled to sulfate reduction (Eq. 4) and mediated by a consortium
91 of anaerobic methane-oxidizing archaea (ANME) and sulfate-reducing bacteria (Knittel and
92 Boetius, 2009; Orphan et al., 2001; Michaelis et al., 2002; Boetius et al., 2000; Hinrichs and
93 Boetius, 2002; Reeburgh, 2007).



95 AOM occurring in the sulfate-reducing zone, fuelled by concurrent methylotrophic
96 methanogenesis activity, i.e., the cryptic methane cycle, could be the reason why methane
97 concentrations are consistently low in sulfidic sediment (Krause and Treude, 2021; Xiao et al.,
98 2017; Xiao et al., 2018). These studies highlight the importance of the cryptic methane cycle
99 on the global methane budget. However, the extent of our knowledge of cryptic methane cycle
100 is restricted to a few aquatic environments. Thus, it is crucial to investigate and understand the
101 cryptic methane cycle in [other aquatic](#) environments to fully understand its impact on the global
102 methane budget. In the present study we focus on organic-rich sediment below oxygen-
103 deficient water in the Santa Barbara Basin (SSB), California.

104 Oxygen minimum zones (OMZ) are regions where high oxygen demand in the water
105 column leads to a dramatic decline or even absence of dissolved oxygen (Wright et al., 2012;
106 Paulmier and Ruiz-Pino, 2009; Wyrтки, 1962; Canfield and Kraft, 2022). In these
107 environments, coastal upwelling of nutrients results in high phytoplankton growth, greatly
108 enhancing organic matter loading and in turn creating a high metabolic oxygen demand during
109 organic matter degradation in the water column. This enhanced respiration depletes oxygen

Deleted: myriad

111 faster than it is replenished (especially in poorly ventilated water bodies), which results in
112 seasonal or continuous low oxygen conditions (Wyrski, 1962; Helly and Levin, 2004; Wright
113 et al., 2012; Levin et al., 2009). Sediment beneath OMZs is typically rich in organic matter
114 supporting predominantly or exclusively anaerobic degradation processes, including
115 methanogenesis (Levin, 2003; Rullkötter, 2006; Middelburg and Levin, 2009; Fernandes et al.,
116 2022; Treude, 2011). Thus, sediments underlying OMZ's are good candidate environments to
117 investigate cryptic methane cycling.

Deleted: strong

118 Located within the Pacific Ocean, between the Channel Islands and the mainland of
119 Santa Barbara, California, USA, the SBB is characterized as a thermally stratified, coastal
120 marine basin with a maximum water column depth of approximately 590 m (Soutar and Crill,
121 1977; Arndt et al., 1990; Sholkovitz, 1973). Low oxygen concentrations ($<10 \mu\text{M}$) are found
122 in the bottom waters below the sill depth (~475 m) of the SBB (Sholkovitz, 1973; Reimers et
123 al., 1996). The sediment in the SBB have an organic carbon content between 2-6%
124 (Schimmelmann and Kastner, 1993). These characteristics make the SBB a prime study site to
125 find evidence of cryptic methane cycling.

Deleted: s

126 Organic carbon sources for methylotrophic methanogenesis, such as methylamine, are
127 ubiquitous in coastal marine environments (Zhuang et al., 2018; Zhuang et al., 2016; Oren,
128 1990), including marine environments where OMZ's exist (Ferdelman et al., 1997; Gibb et al.,
129 1999). Methylamines are derived from osmolytes, such as glycine and betaine, and are
130 synthesized by phytoplankton (Oren, 1990). However, the abundance of methylamines and
131 how they may be driving cryptic methane cycling in anoxic sediment within OMZ's is virtually
132 unknown. Furthermore, the fate of methane from methylotrophic methanogenesis in the sulfate
133 reduction zone is poorly constrained. Particularly, if cryptic methane cycling is active above
134 the sulfate-methane transition zone, gross production and consumption of methane have likely
135 been underestimated. Therefore, finding evidence for the cryptic methane cycle in the SBB is

Deleted: the

Deleted: are

140 a necessary step towards understanding how carbon is cycled through the sediment of the SBB
141 and other OMZs.

142 In the present study we report biogeochemical evidence of cryptic methane cycling in
143 surface sediment (top ~15 cm) collected along a depth transect crossing the SBB. We applied
144 the radiotracer method from Krause and Treude (2021) to trace the production of methane from
145 mono-methylamine, followed by the anaerobic oxidation of methane to inorganic carbon. We
146 combined this approach with standard radiotracer methods for the detection of AOM and
147 sulfate reduction as well as with analyses of sediment porewater geochemistry.

148

149 **2. Methods.**

150 **2.1. Study site and sediment sampling**

151 Sediment samples were collected during the R/V *Atlantis* expedition AT42-19 in fall
152 2019. Collection was achieved with polycarbonate push cores (30.5 cm long, 6.35 cm i.d.),
153 which were deployed by the ROV *JASON* along a depth transect through the SBB. The depth
154 transect selected for this particular study, was the Northern Deposition Transect 3 (NDT3),
155 with three stations (NDT3-A, -C and -D), as well as the Northern Depositional Radial Origin
156 (NDRO), and the Southern Depositional Radial Origin (SDRO) station, located in the deepest
157 part of the basin. Details on the stations, water column depths and near-seafloor oxygen
158 concentrations are provided in Table 1.

159 **Table 1.** Water column depth, bottom water oxygen concentrations and coordinates of each station sampled during
160 this study.

Station	Depth (m)	Bottom Water Oxygen (μM)	Latitude	Longitude
SDRO	586	0	34.2011	-120.0446
NDRO	580	0	34.2618	-120.0309
NDT3-A	572	9.2	34.2921	-120.0258
NDT3-C	498	5	34.3526	-120.0160
NDT3-D	447	8	34.3625	-120.0150

161
162 After sediment collection, ROV push cores were returned to the surface by an elevator
163 platform. Upon retrieval onboard the R/V *Atlantis*, sediment samples were immediately
164 transported to an onboard cold room (6°C) for further processing of biogeochemical parameters
165 (see details in section 2.2.).

166

167 **2.2. Sediment porewater sampling and sulfate analysis**

168 For porewater analyses, two ROV sediment push cores from each station were sliced
169 in 1-cm increments in the top 10 cm of the sediment, followed by 2-cm increments below.

Deleted: '

171 During sediment sampling, ultra-pure argon was flushed over the sediment to minimize
172 oxidation of oxygen sensitive species. The sliced sediment layers were quickly transferred to
173 argon-flushed 50 mL plastic centrifuge vials and centrifuged at 2300 X g for 20 mins to extract
174 the porewater. Subsequently, 2 mL of porewater was subsampled from the supernatant and
175 frozen at -20 °C for shore-based sulfate analysis by ion chromatography (Metrohm 761)
176 following (Dale et al., 2015). Additional porewater (1 mL) was subsampled for the
177 determination of the concentration of methylamine and other metabolic substrates (see section
178 2.4).

179

180 **2.3. Sediment methane and benthic methane flux analyses**

181 Methane concentration in the sediment was determined from a replicate ROV pushcore.
182 Sediment was sliced at 1-cm increments in the top 10 cm, followed by 2-cm increments below.
183 Two mL of sediment was sampled with a cut-off 3 mL plastic syringe and quickly transferred
184 to 12 mL glass serum vials filled with 5 mL 5% (w/w) NaOH solution. The vials were sealed
185 immediately with a grey butyl rubber stopper and aluminum crimps, shaken thoroughly, and
186 stored upside down at 4 °C. Methane concentrations in the headspace were determined shore-
187 based using a gas chromatograph (Shimadzu GC-2015) equipped with a packed Haysep-D
188 column and flame ionization detector. The column was filled with helium as a carrier gas,
189 flowing at 12 mL per minute and heated to 80 °C. Methane concentrations in the environmental
190 samples were calibrated against methane standards (Scott, [Specialty Gases](#)) with a \pm 5%
191 precision.

192 To determine methane flux out of the sediment and into the water column, 1-2
193 custom-built cylindrical benthic flux chambers (BFC) (Treude et al., 2009) were deployed at
194 each sampling station by the ROV Jason. The BFCs consist of a lightweight fiber-reinforced
195 plastic frame, which holds a cylindrical polycarbonate chamber. Buoyant syntactic foam was
196 attached to the feet of the frame to keep the BFC's from sinking too deep into the soft and

Deleted: y

Deleted: Analyzed

199 poorly consolidated sediments, especially in the deeper stations. Water overlying the
200 enclosed sediment was kept mixed with a stirrer bar rotating below the lid of the chamber.
201 The BFC's were equipped with a syringe sampler holding seven, 50 mL glass syringes (6
202 syringes for sample collection and 1 syringe for freshwater injection). One sample syringe
203 withdrew 50 mL of seawater from the chamber volume at pre-programed time intervals. The
204 seventh syringe was used to inject 50 mL of de-ionized water into the chamber shortly after
205 deployment to calculate the volume from the change in salinity in the overlying seawater
206 recorded by a conductivity sensor (type 5860, Aanderaa Data Instruments, Bergen, NO),
207 according to (Kononets et al., 2021).

208 Seawater samples to determine the methane flux out of the sediments were collected
209 in 26 mL serum glass bottles. The 26 mL serum bottles were acid cleaned, and then
210 combusted at 300 °C prior to BFC seawater sample collection. One to two pellets of solid
211 NaOH were added into each empty 26 mL combusted serum bottle. All empty serum bottles
212 were then flushed with ultra-pure nitrogen gas (Airgas Ultra High Purity Grade Nitrogen,
213 Manufacturer Part #:UHP300) for 5 min, then sealed with autoclaved chlorobutyl stoppers
214 and crimps. Lastly, a vacuum pump was used to evacuate the bottles to a pressure down to
215 <0.05 psi prior to sample collection.

216 Immediately after BFC recovery from the seafloor, approximately 20 mL of seawater
217 sample was transferred into the pre-evacuated, acid cleaned, and combusted 26 mL glass
218 serum bottles through the chlorobutyl stopper using a sterile 23G needle. Pressure within the
219 serum bottle was equalized to atmospheric pressure with the introduction of UHP grade
220 nitrogen. Serum bottles were shaken to dilute the NaOH pellets, which terminated metabolic
221 activity and forced the dissolved methane into the gas headspace. The serum bottles were
222 reweighed after sample collection, to calculate the exact volume of the seawater sample.
223 Methane concentrations in seawater collected from the BFC's were analyzed shipboard by
224 gas chromatography according to Qin et al., 2022.

Deleted: 7

Deleted: 6

Deleted: Prior to BFC seawater sample collection,

Deleted: t

Deleted: washed, rinsed three times using MilliQ filtered DI water

230 Total methane concentration in the headspace was calculated following the ideal gas
231 law Eq. (5),

$$232 \quad n = \frac{PV}{RT} * [CH_4] * \frac{1}{V_{SW}} . \quad [5]$$

233 Where n is the total molar concentration of methane, P is atmospheric pressure, V is the volume
234 of the headspace of serum bottle (which is calculated by 26 mL subtracted by the volume of
235 seawater sample), R is the ideal gas constant, T is temperature in Kelvin (288.15 K), $[CH_4]$ is
236 the methane measured by GC as percentage values in ppm, and V_{SW} is the volume of seawater
237 in the serum vial. The volume of sampled seawater in each serum bottle was calculated by
238 subtracting the mass of the empty serum bottle from the mass of the filled serum bottle,
239 normalized by the density of seawater.

240

241 2.4. Determination of methanogenic substrates in porewater

242 To obtain sediment porewater concentrations of methanogenic substrates
243 (methylamine, methanol, and acetate), 1 mL porewater was extracted from 1-2 cm and 9-10
244 cm depth sections at each station (see section 2.2) and syringe-filtered (0.2 μ m) into pre-
245 combusted (350 °C for 3 hrs) amber glass vials (1.8 mL), which were then closed with a PTFE
246 septa-equipped screw caps and frozen at -80 °C until analyses. Samples were analysed at the
247 Pacific Northwest National Laboratory, Environment and Molecular Sciences Division for
248 metabolomic analysis using proton nuclear magnetic resonance (NMR). Prior to analysis,
249 porewater samples were diluted by 10% (v/v) with an internal standard (5 mM 2,2-dimethyl-
250 2-silapentane-5-sulfonate-d6). All NMR spectra were collected using an 800 MHz Bruker
251 Avance Neo (Tava), with a TCI 800/54 H&F/C/N-D-05 Z XT, and an QCI H-P/C/N-D-05 Z
252 ET extended temperature range CryoProbe. The 1D 1H NMR spectra of all samples were
253 processed, assigned, and analysed by using the Chenomx NMR Suite 8.6 software with
254 quantification based on spectral intensities relative to the internal standard. Candidate
255 metabolites present in each of the complex mixture were determined by matching the chemical

Deleted: Porewater metabolomic analysis

257 shift, J-coupling, and intensity information of experimental NMR signals against the NMR
258 signals of standard metabolites in the Chenomx library. The 1D ^1H spectra were collected
259 following standard Chenomx data collection guidelines, employing a 1D NOESY presaturation
260 experiment (noesypr1d) with 65536 complex points and at least 4096 scans at 298 K. Signal to
261 noise ratios (S/N) were measured using MestReNova 14 with the limit of quantification equal
262 to a S/N of 10 and the limit of detection equal to a S/N of 3. The 90° ^1H pulse was calibrated
263 prior to the measurement of each sample with a spectral width of 12 ppm and 1024 transients.
264 The NOESY mixing time was 100 ms and the acquisition time was 4 s followed by a relaxation
265 delay of 1.5 s during which presaturation of the water signal was applied. Time domain free
266 induction decays (72114 total points) were zero-filled to 131072 total points prior to Fourier
267 transform.

268

269 **2.5. Metabolic activity determinations**

270 One replicate ROV sediment push core (hereafter 'ROV rate push core') from each
271 station was sub-sampled with three mini-cores (20 cm long, 2.6 cm i.d.) for radiotracer
272 incubations according to the whole-core injection method (Jørgensen 1978) to collect
273 quantitative metabolic evidence (sulfate reduction, methanogenesis, methane oxidation) of
274 cryptic methane cycling. The incubation methods are detailed below. [Note that not enough
275 sediment cores were collected at each station to perform replicate radiotracer experiments that
276 would have allowed addressing small-scale spatial variability in ex-situ rates.](#)

277

278 **2.5.1. Sulfate reduction via ^{35}S -Sulfate**

279 Within the same day of collection, one mini-core from each ROV rate push core was
280 used to determine sulfate-reduction rates. Radioactive carrier-free ^{35}S -sulfate ($^{35}\text{S}\text{-SO}_4^{2-}$;
281 dissolved in MilliQ water, injection volume 10 μL , activity 260 KBq, specific activity 1.59
282 TBq mg^{-1}) was injected into the mini core at 1-cm increments and incubated at 6 $^\circ\text{C}$ in the dark

Formatted: Font: 12 pt, Not Italic

283 following (Jørgensen, 1978). Injected sediment cores were stored vertically and incubated for
284 ~6 hrs at 6 °C in the dark. Incubations were stopped by slicing the sediment in 1-cm increments
285 into 50 mL plastic centrifuge tubes containing 20 mL 20% (w/w) zinc acetate solution. Each
286 sediment sample was sealed and shaken thoroughly and stored at -20 °C to halt metabolic
287 activity. For the control samples, sediments were added to zinc acetate solution prior to
288 radiotracer injection. In the home laboratory, sulfate reduction rates were determined using the
289 cold-chromium distillation method (Kallmeyer et al., (2004).

290

291 **2.5.2. Methanogenesis and AOM via ¹⁴C-Mono-Methylamine**

292 This study aimed at determining the activity of methanogenesis from mono-
293 methylamine (MG-MMA) and the subsequent anaerobic oxidation of the resulting methane to
294 inorganic carbon by AOM (AOM-MMA). To accomplish this goal, a mini core from each ROV
295 rate push core was injected with radiolabeled ¹⁴C-mono-methylamine (¹⁴C-MMA; dissolved in
296 1 mL water, injection volume 10 µL, activity 220 KBq, specific activity 1.85-2.22 GBq mmol⁻¹)
297 similar to section 2.5.1. After 24 hrs, the incubation was terminated by slicing the sediment
298 at 1-cm increments into 50 mL wide mouth glass vials filled with 20 mL of 5% NaOH. Five
299 killed control samples were prepared by transferring approximately 5 ml of extra sediment
300 from each station into 50 mL wide mouth vials filled with 20 mL of 5% NaOH prior to
301 radiotracer addition. Sample vials and vials with killed controls were immediately sealed with
302 butyl rubber stoppers and aluminium crimps and shaken thoroughly for 1 min to ensure
303 complete biological inactivity. Vials were stored upside down at room temperature until further
304 processing. In the home laboratory, methane production from ¹⁴C-MMA by MG-MMA and
305 subsequent oxidation of the produced ¹⁴C-methane (¹⁴C-CH₄) by AOM-MMA was determined
306 according to the adapted radiotracer method outlined in (Krause and Treude, 2021).

307 To account for ¹⁴C-MMA potentially bound to mineral surfaces (Wang and Lee, 1993,
308 1994; Xiao et al., 2022), we determined the ¹⁴C-MMA recovery factor (RF) for the sediment
309 from the stations NDT3-C, D and NDRO according to Krause and Treude (2021).

310 Metabolic rates of MG-MMA were calculated according to Eq. 7. Note that natural
311 concentrations of MMA in the SBB sediment porewater were either below detection or
312 detectable, but below the quantification limit (<10 μM) (Table S1). Therefore, MMA
313 concentrations were assumed to be 3 μM to calculate the ex-situ rate of MG-MMA (Eq. 8).

$$314 \quad MG-MMA = \frac{a_{CH_4} + a_{TIC}}{a_{CH_4} + a_{TIC} + \left[\frac{a_{MMA}}{RF}\right]} * [MMA] * \frac{1}{t} \quad [7]$$

315 where *MG-MMA* is the rate of methanogenesis from mono-methylamine (nmol cm⁻³ d⁻¹); *a_{CH4}*
316 is the radioactive methane produced from methanogenesis (CPM); *a_{TIC}* is the radioactive total
317 inorganic carbon produced from the oxidation of methane (CPM); *a_{MMA}* the residual
318 radioactive mono-methylamine (CPM); RF is the recovery factor (Krause and Treude, (2021)
319 ; [*MMA*] is the assumed mono-methylamine concentrations in the sediment (nmol cm⁻³); *t* is
320 the incubation time (d). ¹⁴C-CH₄ and ¹⁴C-TIC sample activity was corrected by respective
321 abiotic activity determined in killed controls.

322 Results from the ¹⁴C-MMA incubations were also used to estimate the AOM-MMA
323 rates according to Eq. 8,

$$324 \quad AOM-MMA = \frac{a_{TIC}}{a_{CH_4} + a_{TIC}} * [CH_4] * \frac{1}{t} \quad [8]$$

325 where *AOM-MMA* is the rate of anaerobic oxidation of methane based on methane produced
326 from MMA (nmol cm⁻³d⁻¹); *a_{TIC}* is the produced radioactive total inorganic carbon (CPM); *a_{CH4}*
327 is the residual radioactive methane (CPM); [*CH₄*] is the sediment methane concentration (nmol
328 cm⁻³); *t* is the incubation time (d). ¹⁴C-TIC activity was corrected by abiotic activity determined
329 by replicate dead controls.

330

331 2.5.3 Anaerobic oxidation of methane via ¹⁴C-Methane

Deleted: 8

333 AOM rates from ^{14}C -CH₄ (AOM-CH₄) were determined by injecting radiolabeled ^{14}C -
334 CH₄ (dissolved in anoxic MilliQ, injection volume 10 μL , activity 5 KBq, specific activity
335 1.85–2.22 GBq mmol⁻¹) into one mini core from each ROV rate core at 1-cm increments similar
336 to section 2.5.1. Incubations of the mini cores were stopped after ~24 hours similar to section
337 2.5.2. In the laboratory, AOM-CH₄ was analysed using oven combustion (Treude et al., 2005)
338 and acidification/shaking (Joye et al., 2004). The radioactivity was determined by liquid
339 scintillation counting. AOM-CH₄ rates were calculated according to Eq. 8.

340

341 *2.5.4 Rate constants for AOM-CH₄, MG-MMA, and AOM-MMA*

342

343 [Metabolic rate constants \(k\) for AOM-CH₄, MG-MMA and AOM-MMA were calculated for](#)
344 [relative turnover comparisons using the experimental data determined by sections 2.5.2 and](#)

345 [2.5.3.](#) The rate constants consider the metabolic reaction products, divided by the sum of
346 reaction reactants and products and by time. The metabolic rate constants for AOM-CH₄, MG-
347 MMA and AOM-MMA were calculated according to Eq. 9,

$$348 \quad k = \frac{a_{\text{products}}}{a_{\text{products}} + a_{\text{reactants}}} * \frac{1}{t} \quad [9]$$

349 where k is the metabolic rate constant (day⁻¹); a_{products} is the radioactivity (CPM) of the
350 metabolic reaction products; $a_{\text{reactants}}$ is the radioactivity (CPM) of the metabolic reaction
351 reactants; t is time in days.

352

Formatted: Font: 12 pt

Deleted: Metabolic rate constants (k) for AOM-CH₄, MG-MMA and AOM-MMA were calculated using the experimental data determined by sections 2.5.2 and 2.5.3.

356 **3. Results**

357 **3.1. Sediment biogeochemistry**

358 At most stations, porewater methane concentrations in the top 10-20 cm of sediment
359 fluctuated between 3 and 13 μM with no clear trend (Fig. 1A, E, I, M, and Q). At NDRO,
360 methane steadily increased below 12 cm, reaching 16 μM at 14–15 cm (Fig. 1E). Methane
361 concentrations determined in water samples from the BFC incubations revealed only minor
362 fluctuations over time with no clear trends, suggesting no net fluxes of methane into or out of
363 the sediment at all stations (Fig. 1S). It is notable, however, that the BFCs captured higher
364 methane concentrations (350-800 nM) in the supernatant of station SDRO, NDRO, and NDT3-
365 A compared to NDT3-C and NDT3-D (< 130 nM). Sulfate concentrations showed no strong
366 decline with depth at any station (except maybe a weak tendency at SDRO and NDT3-A) and
367 fluctuated between 23 and 30 mM in the sampled top 10-20 cm (Fig. 1A, E, I, M, and Q).

368 Table S1 provides porewater concentrations of organic carbon sources from the
369 metabolomic analysis, as measured by NMR, that are known to support methanogenesis.
370 Methylamine was detected at SDRO and NDT3-A (1–2 cm), but those concentrations were
371 below the quantification limit (10 μM). Otherwise, methylamine was below detection (<3 μM)
372 for all other samples. Similarly, methanol was detected but below quantification at NDT3-A
373 (1–2 cm) but otherwise below detection. Acetate was at a quantifiable level (21 μM) at NDT3-
374 A (1–2 cm) but was otherwise either below quantification (SDRO, 1-2 cm; NDRO, 1-2 cm) or
375 below detection.

376

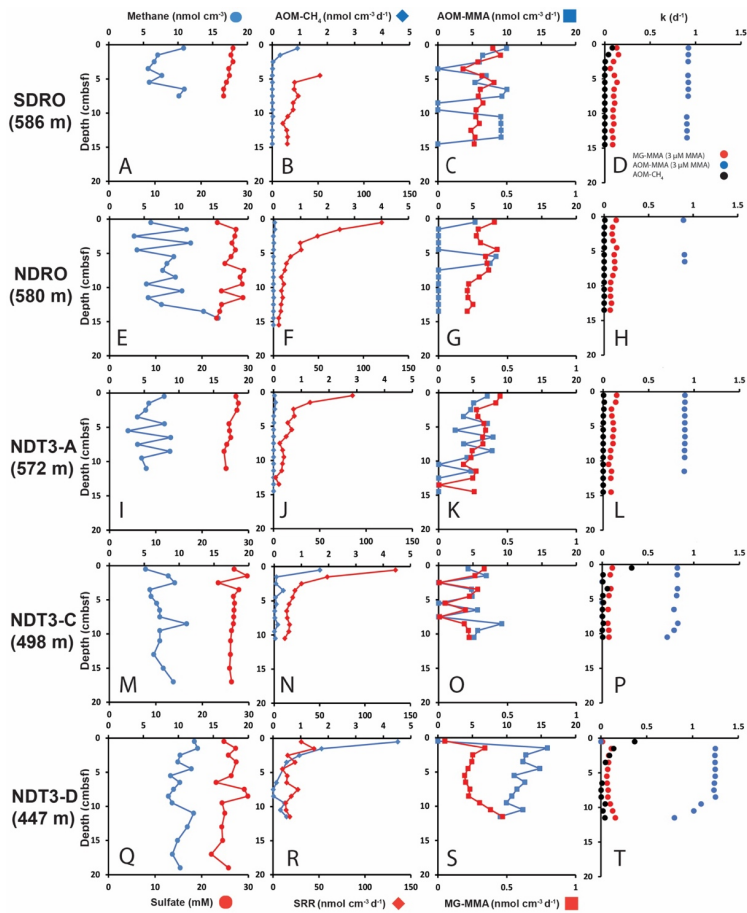
377 **3.2 AOM from ^{14}C -methane and sulfate reduction from ^{35}S -sulfate**

378 Fig. 1B, F, J, N, and R depicts ex-situ rates of AOM- CH_4 and sulfate reduction from
379 the radiotracer incubations with ^{14}C -methane and ^{35}S -sulfate in sediment mini cores,
380 respectively. AOM- CH_4 activity tended to increase with decreasing water depth in the top 5
381 cm of the sediment (from max 0.05 $\text{nmol cm}^{-3} \text{d}^{-1}$ at NDRO to max 4.5 $\text{nmol cm}^{-3} \text{d}^{-1}$ at NDT3-

382 D), while rates were either negligible (SDRO, NDRO, NDT3-A) or $<1 \text{ nmol cm}^{-3} \text{ d}^{-1}$ (NDT3-
383 C, NDT3-D) for depths $>5 \text{ cm}$. Where peaks in AOM were present (SDRO, NDT3-C, NDT3-
384 D) they were always located in the top 0–1 cm sediment layer.

385 Sulfate reduction activity was detected throughout all sediment cores with the highest
386 rates mostly at 0–1 cm, followed by a decrease with increasing sediment depth. The highest
387 individual sulfate reduction peaks were found at NDRO, NDT3-A, and NDT3-C (120, 85 and
388 $133 \text{ nmol cm}^{-3} \text{ d}^{-1}$). At NDT3-D sulfate reduction rates varied between 14 and $45 \text{ nmol cm}^{-3} \text{ d}^{-1}$
389 throughout the core with no clear trend. Note that sulfate reduction data are missing for 0–5
390 cm at SDRO. [due to post-cruise analytical issues](#). Here, rates gradually decreased from 52 to
391 $10 \text{ nmol cm}^{-3} \text{ d}^{-1}$ below 5 cm.

392



393

394 **Figure 1.** Depth profiles of biogeochemical parameters in sediment across the depth transect of the Santa Barbara
 395 Basin. A, E, I, M, and Q: sediment methane and porewater sulfate; B, F, J, N, and R: AOM-CH₄ and sulfate
 396 reduction (determined from direct injection of ¹⁴C-CH₄ and ³⁵S-Sulfate, respectively); C, G, K, O, and S: AOM-
 397 MMA and MG-MMA (determined from direct injection of ¹⁴C-MMA); D, H, L, P, and T: rate constants for AOM-
 398 CH₄, MG-MMA and AOM-MMA.

399 **3.3 Methanogenesis and AOM from ^{14}C -mono-methylamine**

400 **3.3.1 ^{14}C -MMA recovery from sediment**

401 RF values determined in sediments from NDRO, NDT3-C and D stations (see section
402 2.5.2) were 0.93, 0.84, and 0.75, respectively. They were used to correct MG-MMA rates at
403 each station of the study. Note that no RF values were determined for SDRO or the NDT3-A.
404 We applied RF values from NDRO and NDT3-C, respectively, instead.

405

406 **3.3.2 MG-MMA and AOM-MMA**

407 Fig. 1C, G, K, O, S shows ex-situ rates of MG-MMA and AOM-MMA, assuming a
408 natural MMA concentration of $3\ \mu\text{M}$ (see section 2.5.2). At SDRO, NDRO, and NDT3-A, MG-
409 MMA ranged between 0.27 and $0.45\ \text{nmol cm}^{-3}\ \text{d}^{-1}$ throughout the sediment core without trend
410 (Fig. 1C, G, and K). At NDT3-C MG-MMA ex-situ rates were lower ranging between 0.007
411 $\text{nmol cm}^{-3}\ \text{d}^{-1}$ and $0.3\ \text{nmol cm}^{-3}\ \text{d}^{-1}$ without any pattern (Fig. 1O). At NDT3-D, MG-MMA
412 sharply increased from $0.05\ \text{nmol cm}^{-3}\ \text{d}^{-1}$ at $0\text{--}1\ \text{cm}$, to $\sim 0.34\ \text{nmol cm}^{-3}\ \text{d}^{-1}$ at $1\text{--}2\ \text{cm}$. MG-
413 MMA then decreased slightly to $\sim 0.2\ \text{nmol cm}^{-3}\ \text{d}^{-1}$ between 2 and $9\ \text{cm}$, before increasing to
414 $\sim 0.5\ \text{nmol cm}^{-3}\ \text{d}^{-1}$ at the bottom of the core (Fig. 1S).

415 AOM-MMA rates were 1 to 2 orders of magnitude higher than MG-MMA rates and 1
416 to 4 orders of magnitude higher than AOM- CH_4 rates (Fig 1C, G, K, O, S). At SDRO, NDRO,
417 NDT3-A, and NDT3-C, AOM-MMA ex-situ rates ranged between 5.3 and $10\ \text{nmol cm}^{-3}\ \text{d}^{-1}$
418 (unless zero) with no trend (Fig 1C, G, K, and O). At NDT3-D, AOM-MMA rates decreased
419 from $15.9\ \text{nmol cm}^{-3}\ \text{d}^{-1}$ at $1\text{--}2\ \text{cm}$ to $9\ \text{nmol cm}^{-3}\ \text{d}^{-1}$ at $11\text{--}12\ \text{cm}$ (Fig. 1S). At all stations,
420 some sediment intervals showed no biological net AOM-MMA activity (Fig 1C, G, K, O, S).
421 In these sediment intervals, the ^{14}C -TIC activity was statistically not different from the average
422 plus the standard deviation of the killed control samples.

423

424 **3.4 Rate constants for MG-MMA, AOM-MMA and AOM- CH_4**

425 Fig. 1D, H, L, P, and T show the rate constants (k) for MG-MMA, AOM-MMA and
426 AOM-CH₄ for the comparison of relative radiotracer turnover. At all stations, MG-MMA rate
427 constants were between 0.01 and 0.15 d⁻¹. AOM-CH₄ rate constants ranged between 0.0009 d⁻¹
428 and 0.3 d⁻¹. Rate constants for AOM-MMA, however, were considerably higher than MG-
429 MMA and AOM-CH₄ with values ranging between 0.7 and 1.2 d⁻¹. Most rate constants
430 remained constant over depth, with the exemption of AOM-MMA at station NDT3-C and D
431 (Fig. 1P and T), which showed a steady decrease below 9 cm.

432 **4. Discussion**

433

434 **4.1. Evidence of cryptic methane cycling**

435 The aim of the present study was to check for the existence of cryptic methane cycling
436 in SBB surface sediments by presenting evidence for the concurrent activity of sulfate
437 reduction, AOM, and methanogenesis through radiotracer incubations ($^{35}\text{S} -\text{SO}_4^{-2}$, $^{14}\text{C}-\text{CH}_4$,
438 and $^{14}\text{C}-\text{MMA}$, respectively). Our study confirmed indeed that the three processes co-exist at
439 all investigated stations (Fig. 1). The most prominent concurrent metabolic activity was evident
440 from activity peaks near the sediment-water interface at station NDT3-C (Fig. 1N and O). We
441 suggest the concurrent peaking was stimulated by the availability of fresh, i.e., recently
442 deposited, organic matter coinciding with low oxygen concentrations in the bottom water
443 (Table 1). Fresh organic material likely provided a source for both organoclastic sulfate
444 reduction and methylotrophic methanogenesis, and indirectly (i.e., linked to the methane
445 produced) for AOM coupled to either nitrate, iron, or sulfate reduction. Low oxygen
446 concentrations offered favourable conditions for anaerobic processes in the surface sediment.
447 At the remaining stations (SDRO, NDRO, SDT3-A, SDT3-D; Fig. 1), metabolic activity of all
448 three processes was also confirmed near the sediment surface (with the exemption of the
449 missing data for sulfate reduction at SDRO), but they not always depicted rate peaks
450 (particularly not for AOM- CH_4).

451 Methane detected in the sulfate-rich sediment (Fig. 1A, E, I, M, Q) was likely produced
452 by methylotrophic methanogenesis utilizing non-competitive substrates within the sulfate-
453 reducing zone (Oremland and Taylor, 1978; King et al., 1983; Maltby et al., 2016; Maltby et
454 al., 2018; Reeburgh, 2007), which is also indicated by the production of methane from our ^{14}C -
455 MMA incubations. It is interesting to note that methane concentrations remained relatively
456 constant around 5 to 12 μM while AOM- CH_4 tended to increase with decreasing water depth.

457 This pattern suggests that the partial pressure of methane was likely determined by

Deleted: threshold

Deleted: (the Michaelis constant K_m) of AOM

Formatted: Font: 12 pt, Not Italic

460 [thermodynamic equilibrium between methanogenesis and AOM](#) (compare, e.g., with Conrad
461 1999).

462 The finding of [non-linear](#) methane concentrations in surface sediments is against the
463 general view that methane concentrations above the sulfate-methane transition zone show a
464 linear, diffusion-controlled decline towards the sediment-water interface, where methane
465 escapes into the water column (Reeburgh, 2007). We argue that the non-linear methane trends
466 we observe in the present study is an indication for simultaneous methane production and
467 consumption, i.e., cryptic methane cycling, as evident from our radiotracer experiments.

468 [As there is considerable methanogenic activity even at the](#) sediment-water interface (0-
469 1 cm) at all stations, aside from station NDT3-D (Fig. 1C, G, K, O, S), it is conceivable that
470 some methane could diffuse into the water column where it may be oxidized by either aerobic
471 or anaerobic oxidation processes (depending on the presence or absence of oxygen,
472 respectively) before emission into the atmosphere (Reeburgh, 2007). However, benthic
473 chamber incubations at the SBB stations did not indicate a release of methane into the water
474 column (Fig. S1), emphasizing the importance of cryptic methane cycling for preventing the
475 build-up of methane in the surface sediment and its emission into the water column.

476

477 **4.2. Rapid turnover of metabolic substrates**

478 Natural porewater MMA concentrations were mostly below detection (<3 μM);
479 however, in porewater close to the sediment-water interface of SDRO and NDT3-A, MMA
480 was detected but below the quantification limit (<10 μM) (Table S1). Although we are unable
481 to report definitive MMA concentrations, we can bracket the MMA concentrations in a range
482 between 3 and 10 μM . The bracketed MMA concentrations are about 1 to 2 orders of magnitude
483 higher than what has been reported from interstitial porewater at other locations. For example,
484 studies of sediment porewater off the coast of Peru found MMA concentrations to be ~ 0.15
485 μM (Wang and Lee, 1990). Similarly, in sediment porewater collected from Buzzards Bay,

Deleted: remained at steady state due to the simultaneous production by methanogenesis and consumption by between AOM, but did not decrease enough to reach the threshold partial pressure at which AOM activity would stop (the Michaelis constant K_m)

Deleted: and methanogenesis

Deleted: relatively constant

Deleted: As methanogenesis activity showed considerable activity even at the

Formatted: Font: 12 pt

494 Massachusetts and in the Eastern Tropical North Pacific Ocean, MMA concentrations were
495 either present at trace amounts or below detection limit ($<0.05 \mu\text{M}$) (Lee and Olson, 1984).
496 Detectable but low methylamine concentrations in the porewater found in our study could
497 imply that methylamines are rapidly consumed by microbiological processes and/or removed
498 from the porewater through binding to minerals (Wang and Lee, 1990; Wang and Lee, 1993;
499 Xiao et al., 2022). Our study provided support for both hypotheses as we detected the biological
500 potential for MMA consumption via radiotracer (^{14}C -MMA) experiments (Fig. 1) and detected
501 the binding of 7-25% the injected ^{14}C -MMA to sediment (see 3.3.1).

502 Porewater methanol concentrations in the present study were also mainly below
503 detection, except for one sample, where it was not quantifiable (NDT3-A, 1–2 cm; Table S1).
504 In the marine environment, methanol is known to be a non-competitive substrate for
505 methanogenesis (King et al., 1983; Oremland and Taylor, 1978). However, a recent study
506 demonstrated that methanol is a carbon source for a wide variety of metabolisms, including
507 sulfate-reducing and denitrifying bacteria, as well as aerobic and anaerobic methylotrophs
508 (Fischer et al., 2021), which could all be present in the SBB sediments keeping methanol
509 concentrations low. Acetate was also detected in the metabolomic analysis but mostly below
510 quantification (except NDT3-A, 1–2 cm; Table S1). Acetate is formed through fermentation
511 reactions or through homoacetogenesis (Jørgensen, 2000; Ragsdale and Pierce, 2008). It is a
512 favourable food source for many bacteria and archaea such as sulfate reducers and
513 methanogens (Jørgensen, 2000; Conrad, 2020), which would explain its low concentration in
514 the SBB sediments. Low concentrations of the abovementioned metabolites are likely
515 signatures of rapid metabolic turnover, similar to what has been described for microbial
516 utilization of hydrogen in sediment (Conrad, 1999; Hoehler et al., 2001). In this situation,
517 metabolites would be kept at a steady-state concentration close to the thermodynamic
518 equilibrium of the respective consumers.

519

Deleted: porewater

Deleted:

Deleted: nmol g dry wt⁻¹

523 **4.3. Competitive methylamine turnover by non-methanogenic pathways**

524 Large disparities were found between AOM rates determined from the direct injection
525 of ^{14}C - CH_4 (i.e., AOM- CH_4) and AOM determined from the production of ^{14}C -TIC in the ^{14}C -
526 MMA incubations (i.e., AOM-MMA). AOM- CH_4 was roughly 1-2 orders of magnitude lower
527 compared to AOM-MMA (compare Fig. 1 B/C, F/G, J/K, N/O, R/S), indicating that AOM rates
528 determined via ^{14}C -MMA incubations were overestimated. We hypothesize that this disparity
529 is the result of the direct conversion of ^{14}C -MMA to ^{14}C -TIC by processes other than AOM
530 coupled to MG-MMA. Any process converting ^{14}C -MMA directly to ^{14}C -TIC would inflate
531 the rate constant only slightly for MG-MMA, but dramatically for AOM-MMA (see Eq. 8, 9,
532 and 10). Fig. 1D, H, L, P, and T confirm that the rate constants for AOM-MMA are 1 to 2
533 orders of magnitude higher compared to AOM- CH_4 and MG-MMA. [We interpret the](#)
534 [difference in these](#) rate constants [to](#) strongly suggests that the ^{14}C -TIC detected in the analysis
535 of samples incubated with ^{14}C -MMA must result not only from AOM involved in the cryptic
536 methane cycle but also from direct methylamine oxidation by a different anaerobic
537 methylotrophic metabolism that could not be disambiguated using the adapted radiotracer
538 method.

Deleted: T

539 Methylamines are the simplest alkylated amine. [They are](#) derived from the degradation
540 of choline and betaine found in plant and phytoplankton biomass (Oren, 1990; Taubert et al.,
541 2017). The molecules are ubiquitously found in saline and hypersaline conditions in the marine
542 environment (Zhuang et al., 2016; Zhuang et al., 2017; Mausz and Chen, 2019). The
543 importance of methylamine as a nitrogen and carbon source for microbes to build biomass has
544 been well documented (Taubert et al., 2017; Capone et al., 2008; Anthony, 1975; Mausz and
545 Chen, 2019). Methylamines can be metabolized by aerobic methylotrophic bacteria (Taubert
546 et al., 2017; Chistoserdova, 2015; Hanson and Hanson, 1996) and by methylotrophic
547 methanogens anaerobically (Chistoserdova, 2015; Thauer, 1998). [Based on the data reported](#)

Deleted: Here we hypothesize

Deleted: believe

550 [in the present study, we suggest](#) that, in addition to methylotrophic methanogenesis, sulfate
551 reduction was involved in MMA consumption in surface sediment of the SBB.

552 Recent literature does implicate anaerobic methylamine oxidation by sulfate reduction.
553 For example, Cadena et al. (2018) performed in vitro incubations with microbial mats collected
554 from a hypersaline environment with various competitive and non-competitive substrates
555 including tri-methylamine. Microbial mats incubated with trimethylamine stimulated
556 considerable methane production; but after 20 days, H₂S began to accumulate and plateaued
557 after 40 days, suggesting that trimethylamine is not exclusively shuttled to methylotrophic
558 methanogenesis. The molecular data reported in Cadena et al. (2018), however, could not
559 identify a particular group of sulfate-reducing bacteria that proliferated by the addition of
560 trimethylamine. Instead, their molecular data suggested potentially other, non-sulfate reducing
561 bacteria, such as those in the family *Flavobacteriaceae* to be responsible for trimethylamine
562 turnover.

563 Zhuang et al., (2019) investigated heterotrophic metabolisms of C1 and C2 low
564 molecular weight compounds in anoxic sediment collected in the Gulf of Mexico. Sediment
565 was incubated with a variety of ¹⁴C radiotracers alone and in combination with molybdate, a
566 known sulfate reducer inhibitor, to elucidate the metabolic turnover of low molecular weight
567 compounds, including ¹⁴C-labeled trimethylamine. Their results showed that although
568 methylamines did stimulate methane production, radiotracer incubations with molybdate and
569 methylamine demonstrated the inhibition of direct oxidation of ¹⁴C-methylamine to ¹⁴C-CO₂,
570 suggesting that methylamines were simultaneously oxidized to inorganic carbon by non-
571 methanogenic microorganisms. This finding further suggests a competition between
572 methanogens and sulfate-reducing bacteria for methylamine; however, the authors could not
573 rule out AOM as a potential contributor to the inorganic carbon pool.

574 Kivenson et al., (2021) discovered dual genetic code expansion in sulfate-reducing
575 bacteria from sediment within a deep-sea industrial waste dumpsite in the San Pedro Basin,

577 California, which potentially allows the metabolization of trimethylamine. The authors
578 expanded their study to revisit metagenomic and metatranscriptomic data collected from the
579 Baltic Sea and in the Columbia River Estuary and found expression of trimethylamine
580 methyltransferase in Deltaproteobacteria. This result suggested that a trimethylamine
581 metabolism does exist in sulfate-reducing bacteria which was enabled by the utilization of
582 genetic code expansion. Furthermore, the results also suggest that trimethylamine could be the
583 subject of competition between sulfate-reducing bacteria and methylotrophic methanogens.

584 Although the evidence of sulfate-reducing bacteria playing a larger role in methylamine
585 utilization is growing, there are other methylotrophic microorganisms in anaerobic settings that
586 could also be responsible for degrading methylamines. De Anda et al. (2021) discovered and
587 classified a new phylum called Brockarchaeota. The study reconstructed archaeal metagenome-
588 assembled genomes from sediment near hydrothermal vent systems in the Guaymas Basin,
589 Gulf of California, Mexico. Their findings showed that some Brockarchaeota are capable of
590 assimilating trimethylamines, by way of the tetrahydrofolate methyl branch of the Wood-
591 Ljungdahl pathway and the reductive glycine pathway, bypassing methane production in
592 anoxic sediment.

593 Farag et al. (2021) found genomic evidence of a novel Asgard Phylum called
594 *Sifarchaeota* in deep marine sediment off the coast of Costa Rica. The study used comparative
595 genomics to show a cluster, *Candidatus* Odinarchaeota within the *Sifarchaeota* Phylum, which
596 contains genes encoding for an incomplete methanogenesis pathway that is coupled to the
597 carbonyl branch of the Wood-Ljungdahl pathway. The results suggest that this cluster could be
598 involved with utilizing methylamines. The *Sifarchaeota* metagenome-assembled genomes
599 results found genes for nitrite reductase and sulfate adenylyltransferase and phosphoadenosine
600 phosphosulfate reductase, indicating *Sifarchaeota* could perform nitrite and sulfate reduction.
601 However, their study did not directly link nitrite and sulfate reduction to the utilization of
602 methylamines by *Sifarchaeota*.

Deleted: ha

Deleted: But

605 Molecular analysis was not performed in the present study; therefore, we are unable to
606 directly link sulfate-reducing or any other heterotrophic bacteria to the direct anaerobic
607 oxidation of methylamine in the SBB. Future work should combine available geochemical and
608 molecular tools to piece together the complexity of metabolisms involved with methylamine
609 turnover and how it may affect the cryptic methane cycle. We note that there appears to be a
610 growing paradigm shift in the understanding of the utilization of non-competitive substrates in
611 anoxic sediment by sulfate-reducing bacteria and methylotrophic methanogens (including
612 other supposedly non-competitive methanogenic substrates like methanol (Sousa et al., 2018;
613 Fischer et al., 2021)). Apparently, methanogens are in fact able to convert these substrates into
614 methane in the presence of their competitors. Which factors provide them this capability should
615 be the subject of future research.

616

617 ***4.4. Implications for cryptic methane cycling in SBB***

618 The SBB is known to have a network of hydrocarbon cold seeps, where methane and
619 other hydrocarbons are released from the lithosphere into the hydro- and atmosphere either
620 perennially or continuously (Hornafius et al., 1999; Leifer et al., 2010; Boles et al., 2004). The
621 migration of methane and other hydrocarbons vertically into the hydrosphere occur along
622 channels that are focused and permeable, such as fault lines and fractures (Moretti, 1998;
623 Smeraglia et al., 2022). Local tectonics and earthquakes could create new fault lines or fractures
624 that reshape or redisperse less permeable sediments, which may open or close migration
625 pathways for hydrocarbons, including methane (Smeraglia et al., 2022). In fact it has been
626 shown that hydrocarbons move much more efficiently through faults when the region in
627 question is seismically active on time scales <100000 yrs (Moretti, 1998). Given the current
628 and historical seismic activity (Probabilities, 1995) and faulting (Boles et al., 2004) within and
629 surrounding the SBB, it is conceivable that hydrocarbon seep patterns and seepage pathways
630 could also shift over time. A potential consequence of this shifting in the SBB is that methane

631 seepage could spontaneously flow through prior non-seep surface sediment. The fate of this
632 methane would then fall on the methanotrophic communities that are part of the cryptic
633 methane cycle. However, it is not well understood how quickly anaerobic methanotrophs could
634 handle this shift due to their extremely slow growth rates (Knittel and Boetius, 2009; Wilfert
635 et al., 2015; Nauhaus et al., 2007; Dale et al., 2008a). After gaining a better understanding of
636 cryptic methane cycling in the SBB presented in this study, a hypothesis worth testing in future
637 studies is whether cryptic methane cycling based on methylotrophic methanogenesis primes
638 surface sediments to respond faster to increases in methane transport through the sediment.

639 **5. Conclusions**

640 In the present study, we set about to find evidence of cryptic methane cycling in the
641 sulfate-reduction zone of sediment along a depth transect in the oxygen-deficient SBB using a
642 variety of biogeochemical analytics. We found that, within the top 10-20 cm, low methane
643 concentrations were present within sulfate-rich sediment and in the presence of active sulfate
644 reduction. The low methane concentrations were attributed to the balance between
645 methylotrophic methanogenesis and subsequent consumption of the produced methane by
646 AOM. Our results therefore provide strong evidence of cryptic methane cycling in the SBB.
647 We conclude that this important, yet overlooked, process maintains low methane
648 concentrations in surface sediments of this OMZ, and future work should consider cryptic
649 methane cycling in other OMZ's to better constrain carbon cycling in these expanding marine
650 environments.

651 Our radiotracer analyses further indicated microbial activity that oxidizes
652 monomethylamine directly to CO₂ thereby bypassing methane production. Based off the sulfate
653 reduction activity and methylamine consumption to CO₂ detected in this study and the
654 metagenomic clues presented in the literature, we hypothesize that sulfate reduction may also
655 be supported by methylamines. Our study highlights the metabolic complexity and versatility
656 of anoxic marine sediment near the sediment-water interface within the SBB. Future work
657 should consider how methylamines are consumed by different groups of bacteria and archaea,
658 how methylamine utility by other anaerobic methylotrophs affects the cryptic methane cycle
659 and evaluate if potential environmental changes affect the cryptic methane cycle activity.

660

661 **Data Availability Statement**

662 Porewater sulfate concentrations and sulfate reduction rates are accessible through the
663 Biological & Chemical Oceanography Data Management Office (BCO-DMO) under the
664 following DOI's:

665 http://dmoserv3.bco-dmo.org/jg/serv/BCO-DMO/BASIN/porewater_geochemistry.html0,

666 http://dmoserv3.bco-dmo.org/jg/serv/BCO-DMO/BASIN/sediment_parameters.html0,

667 http://dmoserv3.bco-dmo.org/jg/serv/BCO-DMO/BASIN/microbial_activity.html0.

668 Sediment methane concentrations and rates and rate constant data of AOM and methanogenesis
669 can be found in the supplementary material Table S2.

670

671 **Author Contributions**

672 SK and TT designed the study; SK, JL, DY, DR, DH, QQ, FW, and FJ performed experiments
673 and made measurements; SK, JL, DY, DR, DH, QQ, FW, FJ, DV, and TT analysed the data;
674 SK and TT wrote the manuscript draft with input from all co-authors.

675

676 **Competing Interests**

677 Some authors are members of the editorial board of Biogeoscience. The peer-review process
678 was guided by an independent editor, and the authors have also no other competing interests to
679 declare.

680 **Acknowledgements**

681 We thank the captain and crew of R/V Atlantis, the crew of ROV Jason, the crew of AUV
682 Sentry, and the science party of the research cruise AT42-19 for their technical and logistical
683 support. This work was supported by the National Science Foundation NSF Award NO.: EAR-
684 1852912, OCE-1829981 (to TT), and OCE-1830033 (to DV).

685

686 **References**

687

- 688 Anthony, C.: The biochemistry of methylotrophic micro-organisms, *Science Progress* (1933-),
689 167-206, 1975.
- 690 Arndt, S., Lange, C. B., and Berger, W. H.: Climatically controlled marker layers in Santa
691 Barbara Basin sediments and fine-scale core-to-core correlation, *Limnology and*
692 *Oceanography*, 35, 165-173, 1990.
- 693 Barnes, R. and Goldberg, E.: Methane production and consumption in anoxic marine
694 sediments, *Geology*, 4, 297-300, 1976.
- 695 Beulig, F., Røy, H., McGlynn, S. E., and Jørgensen, B. B.: Cryptic CH₄ cycling in the sulfate-
696 methane transition of marine sediments apparently mediated by ANME-1 archaea,
697 *The ISME journal*, <https://doi.org/10.1038/s41396-41018-40273-z>, 2018.
- 698 Boetius, A., Ravensschlag, K., Schubert, C. J., Rickert, D., Widdel, F., Giesecke, A., Amann, R.,
699 Jørgensen, B. B., Witte, U., and Pfannkuche, O.: A marine microbial consortium
700 apparently mediating anaerobic oxidation of methane, *Nature*, 407, 623-626, 2000.
- 701 Boles, J. R., Eichhubl, P., Garven, G., and Chen, J.: Evolution of a hydrocarbon migration
702 pathway along basin-bounding faults: Evidence from fault cement, *AAPG bulletin*, 88,
703 947-970, 2004.
- 704 Cadena, S., García-Maldonado, J. Q., López-Lozano, N. E., and Cervantes, F. J.: Methanogenic
705 and sulfate-reducing activities in a hypersaline microbial mat and associated
706 microbial diversity, *Microbial ecology*, 75, 930-940, 2018.
- 707 Canfield, D. E. and Kraft, B.: The 'oxygen' in oxygen minimum zones, *Environmental*
708 *Microbiology*, 24, 5332-5344, 2022.
- 709 Capone, D. G., Bronk, D. A., Mulholland, M. R., and Carpenter, E. J.: Nitrogen in the marine
710 environment, Elsevier 2008.
- 711 Chistoserdova, L.: Methylotrophs in natural habitats: current insights through
712 metagenomics, *Applied microbiology and biotechnology*, 99, 5763-5779, 2015.
- 713 Conrad, R.: Contribution of hydrogen to methane production and control of hydrogen
714 concentrations in methanogenic soils and sediments, *FEMS microbiology Ecology*,
715 28, 193-202, 1999.
- 716 Conrad, R.: Importance of hydrogenotrophic, aceticlastic and methylotrophic
717 methanogenesis for methane production in terrestrial, aquatic and other anoxic
718 environments: a mini review, *Pedosphere*, 30, 25-39, 2020.
- 719 Dale, A. W., Van Cappellen, P., Aguilera, D., and Regnier, P.: Methane efflux from marine
720 sediments in passive and active margins: Estimations from bioenergetic reaction-
721 transport simulations, *Earth and Planetary Science Letters*, 265, 329-344, 2008a.

722 Dale, A. W., Regnier, P., Knab, N. J., Jørgensen, B. B., and Van Cappellen, P.: Anaerobic
723 oxidation of methane (AOM) in marine sediments from the Skagerrak (Denmark): II.
724 Reaction-transport modeling, *Geochim. Cosmochim. Acta*, 72, 2880-2894, 2008b.

725 Dale, A. W., Sommer, S., Lomnitz, U., Montes, I., Treude, T., Liebetrau, V., Gier, J., Hensen,
726 C., Dengler, M., Stolpovsky, K., Bryant, L. D., and Wallmann, K.: Organic carbon
727 production, mineralisation and preservation on the Peruvian margin, *Biogeosciences*,
728 12, 1537-1559, 2015.

729 De Anda, V., Chen, L.-X., Dombrowski, N., Hua, Z.-S., Jiang, H.-C., Banfield, J. F., Li, W.-J., and
730 Baker, B. J.: Brockarchaeota, a novel archaeal phylum with unique and versatile
731 carbon cycling pathways, *Nature communications*, 12, 1-12, 2021.

732 Farag, I. F., Zhao, R., and Biddle, J. F.: "Sifarchaeota," a Novel Asgard Phylum from Costa
733 Rican Sediment Capable of Polysaccharide Degradation and Anaerobic
734 Methylotrophy, *Applied and environmental microbiology*, 87, e02584-02520, 2021.

735 Ferdelman, T. G., Lee, C., Pantoja, S., Harder, J., Bebout, B. M., and Fossing, H.: Sulfate
736 reduction and methanogenesis in a Thioploca-dominated sediment off the coast of
737 Chile, *Geochimica et Cosmochimica Acta*, 61, 3065-3079, 1997.

738 Fernandes, S., Mandal, S., Sivan, K., Peketi, A., and Mazumdar, A.: Biogeochemistry of
739 Marine Oxygen Minimum Zones with Special Emphasis on the Northern Indian
740 Ocean, *Systems Biogeochemistry of Major Marine Biomes*, 1-25, 2022.

741 Fischer, P. Q., Sánchez-Andrea, I., Stams, A. J., Villanueva, L., and Sousa, D. Z.: Anaerobic
742 microbial methanol conversion in marine sediments, *Environmental microbiology*,
743 23, 1348-1362, 2021.

744 Gibb, S. W., Mantoura, R. F. C., Liss, P. S., and Barlow, R. G.: Distributions and
745 biogeochemistries of methylamines and ammonium in the Arabian Sea, *Deep Sea
746 Research Part II: Topical Studies in Oceanography*, 46, 593-615, 1999.

747 Hanson, R. S. and Hanson, T. E.: Methanotrophic bacteria, *Microbiol. Rev.*, 60, 439-471,
748 1996.

749 Helly, J. J. and Levin, L. A.: Global distribution of naturally occurring marine hypoxia on
750 continental margins, *Deep Sea Research Part I: Oceanographic Research Papers*, 51,
751 1159-1168, 2004.

752 Hinrichs, K.-U. and Boetius, A.: The anaerobic oxidation of methane: new insights in
753 microbial ecology and biogeochemistry, in: *Ocean Margin Systems*, edited by: Wefer,
754 G., Billett, D., Hebbeln, D., Jørgensen, B. B., Schlüter, M., and Van Weering, T.,
755 Springer-Verlag, Berlin, 457-477, 2002.

756 Hoehler, T. M., Alperin, M. J., Albert, D. B., and Martens, C. S.: Apparent minimum free
757 energy requirements for methanogenic Archaea and sulfate-reducing bacteria in an
758 anoxic marine sediment, *FEMS Microbiol. Ecol.*, 38, 33-41, 2001.

759 Hornafius, J. S., Quigley, D., and Luyendyk, B. P.: The world's most spectacular marine
760 hydrocarbon seeps (Coal Oil Point, Santa Barbara Channel, California): Quantification
761 of emissions, *Journal of Geophysical Research: Oceans*, 104, 20703-20711, 1999.

762 Joye, S. B., Boetius, A., Orcutt, B. N., Montoya, J. P., Schulz, H. N., Erickson, M. J., and Logo,
763 S. K.: The anaerobic oxidation of methane and sulfate reduction in sediments from
764 Gulf of Mexico cold seeps, *Chem. Geol.*, 205, 219-238, 2004.

765 Jørgensen, B. B.: A comparison of methods for the quantification of bacterial sulphate
766 reduction in coastal marine sediments: I. Measurements with radiotracer
767 techniques, *Geomicrobiol. J.*, 1, 11-27, 1978.

768 Jørgensen, B. B.: Bacteria and marine biogeochemistry, in: *Marine biogeochemistry*, edited
769 by: Schulz, H. D., and Zabel, M., Springer Verlag, Berlin, 173-201, 2000.

770 Kallmeyer, J., Ferdelman, T. G., Weber, A., Fossing, H., and Jørgensen, B. B.: A cold
771 chromium distillation procedure for radiolabeled sulfide applied to sulfate reduction
772 measurements, *Limnol. Oceanogr. Methods*, 2, 171-180, 2004.

773 King, G., Klug, M. J., and Lovley, D. R.: Metabolism of acetate, methanol, and methylated
774 amines in intertidal sediments of Lowes Cove, Maine, 45, 1848-1853, 1983.

775 Kivenson, V., Paul, B. G., and Valentine, D. L.: An ecological basis for dual genetic code
776 expansion in marine deltaproteobacteria, *Frontiers in microbiology*, 1545, 2021.

777 Knittel, K. and Boetius, A.: Anaerobic oxidation of methane: progress with an unknown
778 process, *Annu. Rev. Microbiol.*, 63, 311-334, 2009.

779 Kononets, M., Tengberg, A., Nilsson, M., Ekeröth, N., Hylén, A., Robertson, E. K., Van De
780 Velde, S., Bonaglia, S., Rütting, T., and Blomqvist, S.: In situ incubations with the
781 Gothenburg benthic chamber landers: Applications and quality control, *Journal of*
782 *Marine Systems*, 214, 103475, 2021.

783 Krause, S. J. and Treude, T.: Deciphering cryptic methane cycling: Coupling of
784 methylotrophic methanogenesis and anaerobic oxidation of methane in hypersaline
785 coastal wetland sediment, *Geochimica et Cosmochimica Acta*, 302, 160-174, 2021.

786 Kristjansson, J. K., Schönheit, P., and Thauer, R. K.: Different K_s values for hydrogen of
787 methanogenic bacteria and sulfate reducing bacteria: an explanation for the
788 apparent inhibition of methanogenesis by sulfate, *Arch. Microbiol.*, 131, 278-282,
789 1982.

790 Lee, C. and Olson, B. L.: Dissolved, exchangeable and bound aliphatic amines in marine
791 sediments: initial results, *Organic Geochemistry*, 6, 259-263, 1984.

792 Leifer, I., Kamerling, M. J., Luyendyk, B. P., and Wilson, D. S.: Geologic control of natural
793 marine hydrocarbon seep emissions, Coal Oil Point seep field, California, *Geo-Marine*
794 *Letters*, 30, 331-338, 2010.

795 Levin, L.: Oxygen minimum zone benthos: Adaptation and community response to hypoxia,
796 *Oceanogr. Mar. Biol. Ann. Rev.*, 41, 1-45, 2003.

797 Levin, L. A. E., W., Gooday, A. J., Jorissen, F., Middelburg, J. J., Naqvi, S. W. A., Neira, C., and
798 Rabalais, N. N. Z., J.: Effects of natural and human-induced hypoxia on coastal
799 benthos, *Biogeosciences*, 6, 2063–2098, 2009.

800 Lovley, D. R. and Klug, M. J.: Model for the distribution of sulfate reduction and
801 methanogenesis in freshwater sediments, *Geochim. Cosmochim. Acta*, 50, 11-18,
802 1986.

803 Lyu, Z., Shao, N., Akinyemi, T., and Whitman, W. B.: Methanogenesis, *Current Biology*, 28,
804 R727-R732, 2018.

805 Maltby, J., Sommer, S., Dale, A. W., and Treude, T.: Microbial methanogenesis in the sulfate-
806 reducing zone of surface sediments traversing the Peruvian margin, *Biogeosciences*,
807 13, 283–299, 2016.

808 Maltby, J., Steinle, L., Löscher, C. R., Bange, H. W., Fischer, M. A., Schmidt, M., and Treude,
809 T.: Microbial methanogenesis in the sulfate-reducing zone of sediments in the
810 Eckernförde Bay, SW Baltic Sea, *Biogeosciences*, 15, 137– 157, 2018.

811 Mausz, M. A. and Chen, Y.: Microbiology and ecology of methylated amine metabolism in
812 marine ecosystems, *Current Issues in Molecular Biology*, 33, 133-148, 2019.

813 Michaelis, W., Seifert, R., Nauhaus, K., Treude, T., Thiel, V., Blumenberg, M., Knittel, K.,
814 Gieseke, A., Peterknecht, K., Pape, T., Boetius, A., Aman, A., Jørgensen, B. B., Widdel,
815 F., Peckmann, J., Pimenov, N. V., and Gulin, M.: Microbial reefs in the Black Sea
816 fueled by anaerobic oxidation of methane, *Science*, 297, 1013-1015, 2002.

817 Middelburg, J. J. and Levin, L. A.: Coastal hypoxia and sediment biogeochemistry,
818 *Biogeosciences*, 6, 1273-1293, 2009.

819 Moretti, I.: The role of faults in hydrocarbon migration, *Petroleum Geoscience*, 4, 81-94,
820 1998.

821 Nauhaus, K., Albrecht, M., Elvert, M., Boetius, A., and Widdel, F.: In vitro cell growth of
822 marine archaeal-bacterial consortia during anaerobic oxidation of methane with
823 sulfate, *Environ. Microbiol.*, 9, 187-196, 2007.

824 Oremland, R. S. and Polcin, S.: Methanogenesis and sulfate reduction: competitive and
825 noncompetitive substrates in estuarine sediments, *Appl. Environ. Microbiol.*, 44,
826 1270-1276, 1982.

827 Oremland, R. S. and Taylor, B. F.: Sulfate reduction and methanogenesis in marine
828 sediments, *Geochimica et Cosmochimica Acta*, 42, 209-214, 1978.

829 Oremland, R. S., Marsh, L. M., and Polcin, S.: Methane production and simultaneous
830 sulphate reduction in anoxic, salt marsh sediments, *Nature*, 296, 143-145, 1982.

831 Oren, A.: Formation and breakdown of glycine betaine and trimethylamine in hypersaline
832 environments, *Antonie van Leeuwenhoek*, 58, 291-298, 1990.

833 Orphan, V. J., Hinrichs, K.-U., Ussler III, W., Paull, C. K., Tayleur, L. T., Sylva, S. P., Hayes, J. M.,
834 and DeLong, E. F.: Comparative analysis of methane-oxidizing archaea and sulfate-
835 reducing bacteria in anoxic marine sediments, *Appl. Environ. Microbiol.*, 67, 1922-
836 1934, 2001.

837 Paulmier, A. and Ruiz-Pino, D.: Oxygen minimum zones (OMZs) in modern ocean, *Progr.*
838 *Oceanog.*, 80, 113-128, 2009.

839 Probabilities, W. G. o. C. E.: Seismic hazards in southern California: probable earthquakes,
840 1994 to 2024, *Bulletin of the Seismological Society of America*, 85, 379-439, 1995.

841 Qin, Q., Kinnaman, F. S., Gosselin, K. M., Liu, N., Treude, T., and Valentine, D. L.: Seasonality
842 of water column methane oxidation and deoxygenation in a dynamic marine
843 environment, *Geochimica et Cosmochimica Acta*, 336, 219-230, 2022.

844 Ragsdale, S. W. and Pierce, E.: Acetogenesis and the Wood-Ljungdahl pathway of CO₂
845 fixation, *Biochimica et Biophysica Acta (BBA)-Proteins and Proteomics*, 1784, 1873-
846 1898, 2008.

847 Reeburgh, W. S.: Oceanic methane biogeochemistry, *Chem. Rev.*, 107, 486-513, 2007.

848 Reimers, C. E., Ruttenberg, K. C., Canfield, D. E., Christiansen, M. B., and Martin, J. B.:
849 Porewater pH and authigenic phases formed in the uppermost sediments of Santa
850 Barbara Basin, *Geochim. Cosmochim. Acta*, 60, 4037-4057, 1996.

851 Rullkötter, J.: Organic matter: the driving force for early diagenesis, in: *Marine*
852 *geochemistry*, Springer, 125-168, 2006.

853 Schimmelmann, A. and Kastner, M.: Evolutionary changes over the last 1000 years of
854 reduced sulfur phases and organic carbon in varved sediments of the Santa Barbara
855 Basin, California, *Geochimica et Cosmochimica Acta*, 57, 67-78, 1993.

856 Sholkovitz, E.: Interstitial water chemistry of the Santa Barbara Basin sediments, *Geochimica*
857 *et Cosmochimica Acta*, 37, 2043-2073, 1973.

858 Smeraglia, L., Fabbi, S., Billi, A., Carminati, E., and Cavinato, G. P.: How hydrocarbons move
859 along faults: Evidence from microstructural observations of hydrocarbon-bearing
860 carbonate fault rocks, *Earth and Planetary Science Letters*, 584, 117454, 2022.

861 Sousa, D. Z., Visser, M., Van Gelder, A. H., Boeren, S., Pieterse, M. M., Pinkse, M. W.,
862 Verhaert, P. D., Vogt, C., Franke, S., and Kümmel, S.: The deep-subsurface sulfate

863 reducer *Desulfotomaculum kuznetsovii* employs two methanol-degrading pathways,
864 *Nature communications*, 9, 1-9, 2018.

865 Soutar, A. and Crill, P. A.: Sedimentation and climatic patterns in the Santa Barbara Basin
866 during the 19th and 20th centuries, *Geological Society of America Bulletin*, 88, 1161-
867 1172, 1977.

868 Stephenson, M. and Stickland, L. H.: CCVII. Hydrogenase. III. The bacterial formation of
869 methane by the reduction of one-carbon compounds by molecular hydrogen,
870 *Biochem. J.*, 27, 1517–1527, 1933.

871 Taubert, M., Grob, C., Howat, A. M., Burns, O. J., Pratscher, J., Jehmlich, N., von Bergen, M.,
872 Richnow, H. H., Chen, Y., and Murrell, J. C.: Methylamine as a nitrogen source for
873 microorganisms from a coastal marine environment, *Environmental microbiology*,
874 19, 2246-2257, 2017.

875 Thauer, R. K.: Biochemistry of methanogenesis: a tribute to Marjory Stephenson,
876 *Microbiology*, 144, 2377-2406, 1998.

877 Treude, T.: Biogeochemical reactions in marine sediments underlying anoxic water bodies,
878 in: *Anoxia: Paleontological Strategies and Evidence for Eukaryote Survival*, edited by:
879 Altenbach, A., Bernhard, J., and Seckbach, J., *Cellular Origins, Life in Extreme Habitats*
880 *and Astrobiology (COLE) Book Series*, Springer, Dordrecht, 18-38, 2011.

881 Treude, T., Krüger, M., Boetius, A., and Jørgensen, B. B.: Environmental control on anaerobic
882 oxidation of methane in the gassy sediments of Eckernförde Bay (German Baltic),
883 *Limnol. Oceanogr.*, 50, 1771-1786, 2005.

884 Treude, T., Smith, C. R., Wenzhoefer, F., Carney, E., Bernardino, A. F., Hannides, A. K.,
885 Krueger, M., and Boetius, A.: Biogeochemistry of a deep-sea whale fall: sulfate
886 reduction, sulfide efflux and methanogenesis, *Mar. Ecol. Prog. Ser.*, 382, 1-21, 2009.

887 Wang, X.-c. and Lee, C.: The distribution and adsorption behavior of aliphatic amines in
888 marine and lacustrine sediments, *Geochimica et Cosmochimica Acta*, 54, 2759-2774,
889 1990.

890 Wang, X.-C. and Lee, C.: Adsorption and desorption of aliphatic amines, amino acids and
891 acetate by clay minerals and marine sediments, *Marine Chemistry*, 44, 1-23, 1993.

892 Wang, X.-C. and Lee, C.: Sources and distribution of aliphatic amines in salt marsh sediment,
893 *Organic Geochemistry*, 22, 1005-1021, 1994.

894 Wehrmann, L. M., Risgaard-Petersen, N., Schrum, H. N., Walsh, E. A., Huh, Y., Ikehara, M.,
895 Pierre, C., D'Hondt, S., Ferdelman, T. G., and Ravelo, A. C.: Coupled organic and
896 inorganic carbon cycling in the deep seafloor sediment of the northeastern
897 Bering Sea Slope (IODP Exp. 323), *Chemical Geology*, 284, 251-261, 2011.

898 Wilfert, P., Krause, S., Liebetrau, V., Schönfeld, J., Haeckel, M., Linke, P., and Treude, T.:
899 Response of anaerobic methanotrophs and benthic foraminifera to 20 years of
900 methane emission from a gas blowout in the North Sea, *Marine and Petroleum*
901 *Geology*, 68, 731-742, 2015.

902 Winfrey, M. R. and Ward, D. M.: Substrates for sulfate reduction and methane production
903 in intertidal sediments, *Appl. Environ. Microbiol.*, 45, 193-199, 1983.

904 Wright, J. J., Konwar, K. M., and Hallam, S. J.: Microbial ecology of expanding oxygen
905 minimum zones, *Nature Reviews Microbiology*, 10, 381-394, 2012.

906 Wyrski, K.: The oxygen minima in relation to ocean circulation, *Deep Sea Research and*
907 *Oceanographic Abstracts*, 11-23,

908 Xiao, K., Beulig, F., Kjeldsen, K., Jorgensen, B., and Risgaard-Petersen, N.: Concurrent
909 Methane Production and Oxidation in Surface Sediment from Aarhus Bay, Denmark,
910 *Frontiers in Microbiology*, 8, 10.3389/fmicb.2017.01198, 2017.

911 Xiao, K., Beulig, F., Roy, H., Jorgensen, B., and Risgaard-Petersen, N.: Methylotrophic
912 methanogenesis fuels cryptic methane cycling in marine surface sediment,
913 *Limnology and Oceanography*, 63, 1519-1527, 10.1002/lno.10788, 2018.

914 Xiao, K.-Q., Moore, O. W., Babakhani, P., Curti, L., and Peacock, C. L.: Mineralogical control
915 on methylotrophic methanogenesis and implications for cryptic methane cycling in
916 marine surface sediment, *Nature Communications*, 13, 1-9, 2022.

917 Zhuang, G.-C., Montgomery, A., and Joye, S. B.: Heterotrophic metabolism of C1 and C2 low
918 molecular weight compounds in northern Gulf of Mexico sediments: Controlling
919 factors and implications for organic carbon degradation, *Geochimica et*
920 *Cosmochimica Acta*, 247, 243-260, 2019.

921 Zhuang, G.-C., Elling, F. J., Nigro, L. M., Samarkin, V., Joye, S. B., Teske, A., and Hinrichs, K.-
922 U.: Multiple evidence for methylotrophic methanogenesis as the dominant
923 methanogenic pathway in hypersaline sediments from the Orca Basin, Gulf of
924 Mexico, *Geochim. Cosmochim. Acta*, 187, 1-20, 2016.

925 Zhuang, G.-C., Lin, Y.-S., Bowles, M. W., Heuer, V. B., Lever, M. A., Elvert, M., and Hinrichs,
926 K.-U.: Distribution and isotopic composition of trimethylamine, dimethylsulfide and
927 dimethylsulfoniopropionate in marine sediments, *Mar. Chem.*, 196, 35-46, 2017.

928 Zhuang, G.-C., Heuer, V. B., Lazar, C. S., Goldhammer, T., Wendt, J., Samarkin, V. A., Elvert,
929 M., Teske, A. P., Joye, S. B., and Hinrichs, K.-U.: Relative importance of
930 methylotrophic methanogenesis in sediments of the Western Mediterranean Sea,
931 *Geochim. Cosmochim. Acta*, 224, 2018.

932
933